

High-field critical current enhancement by irradiation induced correlated and random defects in $(\text{Ba}_{0.6}\text{K}_{0.4})\text{Fe}_2\text{As}_2$

K. J. Kihlstrom, L. Fang, Y. Jia, B. Shen, A. E. Koshelev, U. Welp, G. W. Crabtree, W.-K. Kwok, A. Kayani, S. F. Zhu, and H.-H. Wen

Citation: *Applied Physics Letters* **103**, 202601 (2013); doi: 10.1063/1.4829524

View online: <http://dx.doi.org/10.1063/1.4829524>

View Table of Contents: <http://scitation.aip.org/content/aip/journal/apl/103/20?ver=pdfcov>

Published by the AIP Publishing

Articles you may be interested in

Realization of practical level current densities in $\text{Sr}_{0.6}\text{K}_{0.4}\text{Fe}_2\text{As}_2$ tape conductors for high-field applications
Appl. Phys. Lett. **104**, 202601 (2014); 10.1063/1.4879557

High, magnetic field independent critical currents in $(\text{Ba},\text{K})\text{Fe}_2\text{As}_2$ crystals
Appl. Phys. Lett. **101**, 012601 (2012); 10.1063/1.4731204

Fluctuation of mean free path and transition temperature induced vortex pinning in $(\text{Ba},\text{K})\text{Fe}_2\text{As}_2$ superconductors
Appl. Phys. Lett. **100**, 212601 (2012); 10.1063/1.4714543

Enhanced critical current properties in $\text{Ba}_{0.6}\text{K}_{0.4+x}\text{Fe}_2\text{As}_2$ superconductor by overdoping of potassium
Appl. Phys. Lett. **98**, 042508 (2011); 10.1063/1.3549195

Effects of proton irradiation on the high-temperature superconducting system $\text{Y}_{1-x}\text{Pr}_x\text{Ba}_2\text{Cu}_3\text{O}_{7-\delta}$
Appl. Phys. Lett. **71**, 3415 (1997); 10.1063/1.120352



2014 Special Topics

PEROVSKITES | 2D MATERIALS | MESOPOROUS MATERIALS | BIOMATERIALS/ BIOELECTRONICS | METAL-ORGANIC FRAMEWORK MATERIALS

AIP | APL Materials

Submit Today!

High-field critical current enhancement by irradiation induced correlated and random defects in $(\text{Ba}_{0.6}\text{K}_{0.4})\text{Fe}_2\text{As}_2$

K. J. Kihlstrom,^{1,2} L. Fang,^{1,a)} Y. Jia,^{1,b)} B. Shen,¹ A. E. Koshelev,¹ U. Welp,¹
 G. W. Crabtree,^{1,2} W.-K. Kwok,¹ A. Kayani,³ S. F. Zhu,⁴ and H.-H. Wen⁵

¹Materials Science Division, Argonne National Laboratory, Argonne, Illinois 60439, USA

²Department of Physics, University of Illinois at Chicago, Chicago, Illinois 60607, USA

³Department of Physics, Western Michigan University, Kalamazoo, Michigan 49008, USA

⁴Physics Division, Argonne National Laboratory, Argonne, Illinois 60439, USA

⁵National Laboratory of Solid State Microstructures, Department of Physics,
 Center for Superconducting Physics and Materials, Nanjing University, Nanjing 210093, China

(Received 19 September 2013; accepted 19 October 2013; published online 11 November 2013)

Mixed pinning landscapes in superconductors are emerging as an effective strategy to achieve high critical currents in high, applied magnetic fields. Here, we use heavy-ion and proton irradiation to create correlated and point defects to explore the vortex pinning behavior of each and combined constituent defects in the iron-based superconductor $\text{Ba}_{0.6}\text{K}_{0.4}\text{Fe}_2\text{As}_2$ and find that the pinning mechanisms are non-additive. The major effect of p-irradiation in mixed pinning landscapes is the generation of field-independent critical currents in very high fields. At $7\text{T} \parallel c$ and 5K , the critical current density exceeds $5\text{MA}/\text{cm}^2$. © 2013 AIP Publishing LLC. [<http://dx.doi.org/10.1063/1.4829524>]

Among the iron-based superconductors, $\text{Ba}_{1-x}\text{K}_x\text{Fe}_2\text{As}_2$ has attracted considerable interest for its materials parameters that are very attractive for potential applications.¹ At optimal doping, $x \sim 0.4$, the superconducting transition temperature, T_c , is as high as $T_c \sim 38\text{K}$,² comparable to MgB_2 , the upper critical field is of the order of 100T (Ref. 3) sufficient for high-field low-temperature applications,¹ and, importantly, the superconducting anisotropy is comparatively low, $\Gamma \sim 2$.^{3,4} Round $\text{Ba}_{1-x}\text{K}_x\text{Fe}_2\text{As}_2$ wires made by the powder-in-tube process showed good grain-to-grain connectivity and promising J_c -values in high magnetic fields.⁵ Furthermore, this material is remarkably resilient to defects introduced, for example, by particle irradiation such as protons or heavy ions.⁶ In contrast to the extensively studied electron-doped companion compound $\text{Ba}(\text{Fe}_{1-x}\text{Co}_x)_2\text{As}_2$,⁷ the superconducting transition temperature of hole-doped $\text{Ba}_{1-x}\text{K}_x\text{Fe}_2\text{As}_2$ is hardly suppressed by proton and heavy ion irradiation, even at high fluences of 8×10^{16} protons/cm² or 1×10^{12} Pb-ions/cm², respectively, making it interesting for magnet applications in high-radiation environments. In addition, the large tolerance to defects offers wide flexibility to engineer diverse vortex pinning structures that support high critical currents. Previous work on cuprate high temperature superconductors has shown that mixed pinning landscapes composed of correlated and random disorder^{8,9} or large and small random pin sites¹⁰ are especially effective for achieving very high in-field critical currents.

Here, we explore the limits of vortex pinning and critical current in $\text{Ba}_{0.6}\text{K}_{0.4}\text{Fe}_2\text{As}_2$ single crystals with tailored correlated and point defects induced by heavy-ion and proton irradiation, respectively. Successive irradiations of the

same sample enable systematic study of the pinning effectiveness and critical current enhancement due to defects introduced by each irradiation step, the differentiation between pinning and self-field effects, and the interaction of pinning by multiple defect types. The critical current increases approximately as the square-root of proton-fluence, and decreases with magnetic field as $1/\sqrt{B}$ indicative of strong vortex pinning by sparse defects. We present a study of vortex pinning by proton-irradiation induced defects in iron-based superconductors on the background of pre-existing columnar defects induced by Pb-ion irradiation and find that the pinning mechanisms are non-additive. The major effect of p-irradiation in mixed pinning landscapes is the generation of field-independent critical currents at very high fields. At $7\text{T} \parallel c$ and 5K , the critical current density of our $\text{Ba}_{0.6}\text{K}_{0.4}\text{Fe}_2\text{As}_2$ single crystals exceeds $5\text{MA}/\text{cm}^2$, a value typical of state-of-the-art $\text{YBa}_2\text{Cu}_3\text{O}_7$ (YBCO) coated conductors.⁹

We report measurements on two $\text{Ba}_{0.6}\text{K}_{0.4}\text{Fe}_2\text{As}_2$ crystals: a pristine sample, crystal A, with dimensions of $0.4 \times 0.6 \times 0.02\text{mm}^3$, and crystal B with dimensions of $0.3 \times 0.6 \times 0.04\text{mm}^3$ which was previously irradiated with 1.4GeV Pb-ions at the Argonne Tandem Linear Accelerator System (ATLAS) facility to a dose matching field of $B_\Phi = 21\text{T}$ ($N \sim 1 \times 10^{12}$ ions/cm²). The two samples were subsequently irradiated along the crystal c-axis at the 6MV tandem accelerator at Western Michigan University with 4MeV protons using beam currents of $\sim 200\text{nA}$. Crystal B underwent three successive proton irradiations: (i) 1×10^{16} p/cm², (ii) 2×10^{16} p/cm², and (iii) 3×10^{16} p/cm², while the pristine crystal A was likewise irradiated in sequential doses of 1×10^{16} p/cm², 3×10^{16} p/cm², and 3×10^{16} p/cm². The superconducting transition temperature and the transition width were determined from magnetization versus temperature measurements performed in $10\text{Oe} \parallel c$ after zero field cooling. The critical current density, J_c , was

^{a)}Current address: Department of Chemistry, Northwestern University, Evanston, Illinois 60208, USA.

^{b)}Current address: Department of Physics and Astronomy, Northwestern University, Evanston, Illinois 60208, USA.

obtained from the magnetization hysteresis, ΔM , using the Bean critical state model, $J_c = 20 \Delta M/[a(1-a/3b)]$, where a and b ($a < b$) are the lateral dimensions of the crystals.¹¹

Irradiation with protons of several MeV in energy typically produces comparatively low energy recoils, ≤ 1 keV.¹² Therefore, the defect structure consists predominantly of point defects of single displaced atoms and small collision cascades, and possibly clusters of point defects. Extensive transmission electron microscopy (TEM) work on proton-irradiated $\text{YBa}_2\text{Cu}_3\text{O}_7$ revealed anisotropic clusters and cascades, both of roughly 2–4 nm in size.¹³ At present, no such studies exist for $\text{Ba}_{0.6}\text{K}_{0.4}\text{Fe}_2\text{As}_2$. Although the details of the irradiation induced defect structure will depend on the material at hand and on the pre-existing defects, we assume here that proton-irradiation of $\text{Ba}_{0.6}\text{K}_{0.4}\text{Fe}_2\text{As}_2$ produces a mixture of point defects, nm-sized cascades and possibly clusters.

The evolution of the superconducting transition of crystals A and B with p-irradiation is presented in Figure 1. For both samples, a cumulative fluence of 6×10^{16} (7×10^{16}) p/cm² yields a suppression of T_c by just ~ 1 K. In contrast, in $\text{Ba}(\text{Fe}_{1-x}\text{Co}_x)_2\text{As}_2$ such T_c -suppression is already reached after a fluence of 0.8×10^{16} p/cm².⁷

The field dependence of the magnetization hysteresis at 5 K of samples A and B at various stages of particle irradiation is summarized in Figure 2. The magnetization hysteresis of the pristine sample (crystal A) displays a sharp peak around zero-field. This feature has been observed in various iron-based superconductors and has been attributed to sparse strong pinning sites.¹⁴ Upon p-irradiation the magnetization hysteresis loops expand uniformly while approximately maintaining their over-all shape. In contrast, crystal B, previously irradiated with 1.4 GeV Pb-ions to a dose matching field of $B_\Phi = 21$ T, shows a very broad magnetization hysteresis loop. The Pb-ion irradiation induces discontinuous amorphous tracks with average diameter of 3.7 nm, which are very effective vortex pinning sites.⁶ The most pronounced effect of p-irradiation on this sample is the enhancement of pinning at high magnetic fields, whereas in low fields the effect is smaller. The magnetization hysteresis of

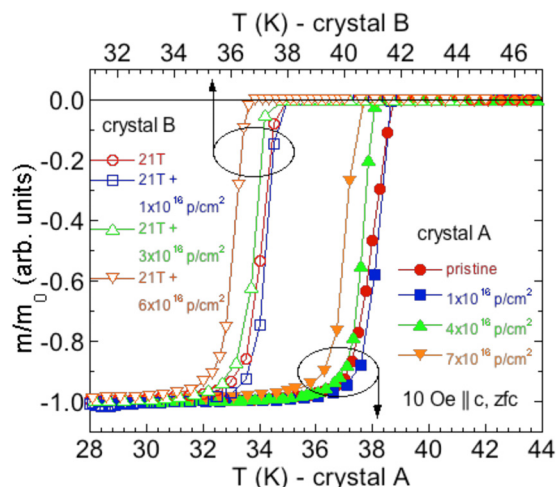


FIG. 1. Superconducting transitions of crystal A (bottom x-axis) and of crystal B (top x-axis) measured in a field of 10 Oe \parallel c on warming after zero-field cooling. The transitions do not broaden upon irradiation.

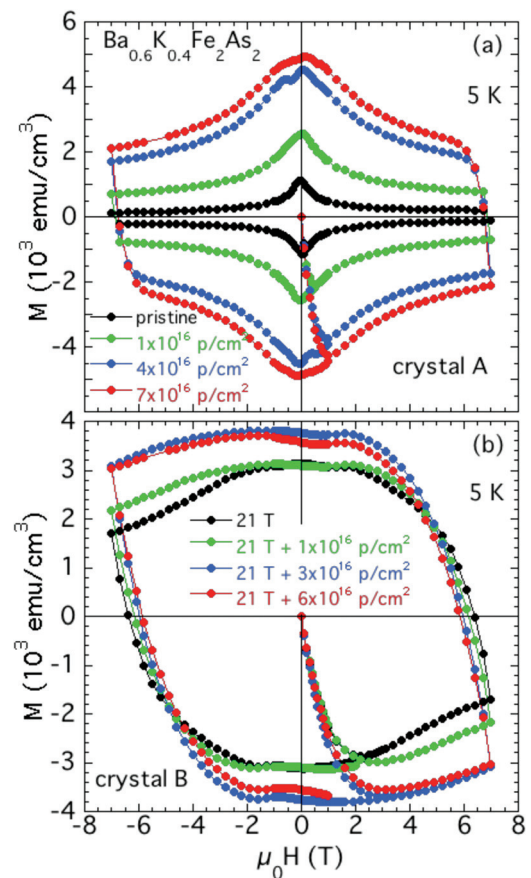


FIG. 2. (a) Field dependence of the magnetization at 5 K of crystal A and crystal B (panel (b)) for various stages of p-irradiation.

crystal B and for crystal A in some runs displays a dip near zero-field. Such feature has been reported before and may be caused by the highly inhomogeneous field distribution in the trapped-field state⁷ and the anisotropy of J_c .¹⁵

Since the reversal of the critical state of sample B and of sample A at high p-fluences occurs over a large field range, we evaluate J_c from the magnetization data between 0 T and -7 T while decreasing the field from 7 T, and from the data between 0 T and 7 T while increasing the field from -7 T, respectively. The large enhancement of J_c of crystal A due to p-irradiation is clearly seen, reaching a factor of 20 at high fields (Fig. 3(a)). After a cumulative fluence of 7×10^{16} p/cm² J_c approaches, values of 6 MA/cm² at 5 K and low fields. Similar values have recently been reported after irradiation with 3 MeV protons to a fluence of 5.3×10^{16} p/cm².¹⁶ The increase of J_c with p-fluence is sub-linear as shown in Fig. 4 for two field values. The observed $J_c(p)$ -dependences are well described with power-laws with exponents 1/2–1/3. These findings are consistent with theoretical models of pinning by isolated random strong pins,^{17,18} which predict that in low magnetic fields J_c should depend on defect concentration n_p as $J_c \sim n_p^\gamma$, where $\gamma \sim 1/2$. In high fields, where single-vortex pinning changes to lattice pinning, the square-root dependence on defect concentration is expected to cross-over into a linear variation¹⁸ and the field dependence of J_c acquires a $1/\sqrt{B}$ variation.^{14,17} On the other hand, the field-dependence seen in experiment approaches the expected $1/\sqrt{B}$ variation (see below), the observed concentration dependence remains sub-linear at all

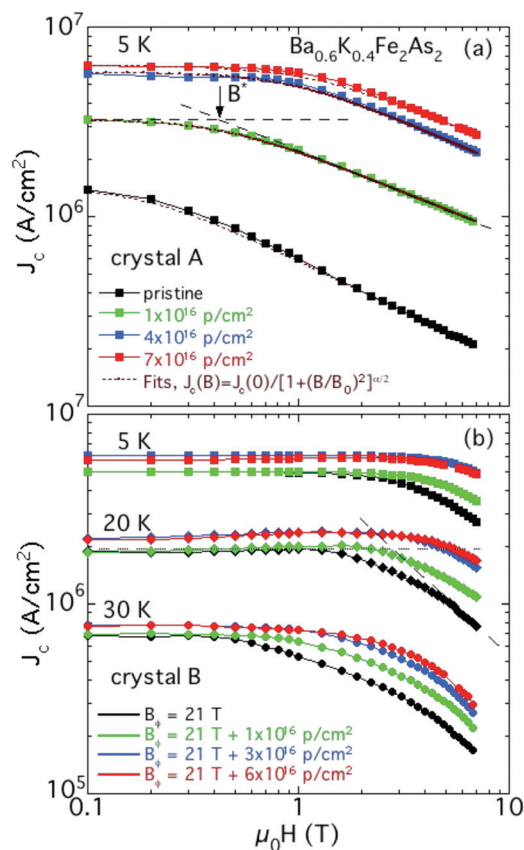


FIG. 3. (a) Field dependence of the critical current density of crystal A at 5 K for various fluences of p-irradiation. (b) Field dependence of the critical current density of crystal B at 5, 20, and 30 K for various fluences of p-irradiation.

measured field values. It is possible that in the experimental field range, we do not completely traverse the cross-over for the high-fluence samples. Furthermore, we assume that the concentration of effective strong pinning sites is proportional to the p-fluence. However, in the absence of detailed TEM work especially the concentration of clusters in

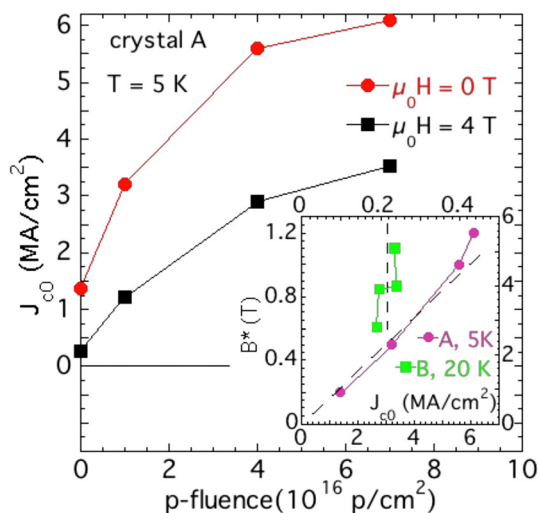


FIG. 4. Dependence of the critical current density of crystal A at zero-field and at 4 T on p-fluence. The inset shows the dependence of the accommodation field B^* on the zero-field critical current density of crystal A at 5 K and of crystal B at 20 K. The data for crystal A are referenced to the lower x-axis and the left y-axis whereas the data for crystal B are referenced to the top x-axis and the right y-axis.

$\text{Ba}_{0.6}\text{K}_{0.4}\text{Fe}_2\text{As}_2$, and the dependence of their nucleation and growth kinetics on p-fluence remains uncertain. In fact, the increase of the residual resistance with p-fluence in $\text{Ba}(\text{Fe}_{1-x}\text{Co}_x)_2\text{As}_2$ was found to be almost linear at optimal doping, whereas the dependence at other compositions was sub-linear.¹⁹

For all p-fluences, the critical current density of crystal A is well described by a relation of the form $J_c \sim B^{-\alpha}$ for $B > B^*$ and $J_c \sim \text{constant}$ for $B < B^*$. The accommodation field B^* is determined from the data as indicated by the arrow in Fig. 3(a). The exponent α decreases from $\alpha = 0.54$ in the pristine sample to $\alpha \sim 0.47$ in the p-irradiated samples. This smooth evolution of the critical current density suggests that the underlying pinning mechanism does not change appreciably due to p-irradiation, namely, pinning by random strong pin sites.

The observation of field-independent J_c at low fields and $J_c \sim 1/\sqrt{B}$ at higher fields has been interpreted as a signature of strong pinning by sparse defects.^{14,17} However, this interpretation of the low-field data and the determination of the intrinsic zero-field critical current $J_c(0)$ are complicated by the fact that different mechanisms are active simultaneously, such as single-vortex pinning and self-field effects.²⁰ The range of nearly field-independent J_c , indicated by the value of B^* , increases systematically with p-irradiation. In fact, as shown in the inset of Fig. 4, B^* is essentially proportional to the apparent zero-field value of the critical current, J_{c0} . This finding suggests that B^* indicates the onset of self-field effects. As has been described in detail earlier,²⁰ in samples with large demagnetization factors strong curvature of vortices causes the critical state in low fields to be established across the thickness, t , of the samples rather than the width. The characteristic field scale associated with this process is $B_s = k\mu_0 J_{c0} t$, where k is a geometry-dependent constant of order unity. With $J_{c0} \sim 6 \text{ MA/cm}^2$ and $t = 20 \mu\text{m}$, a typical field scale of $B_s \sim 1.5 \text{ T}$ can be estimated which is close to the observed values of B^* (see Fig. 3(a)). As the applied field falls below B_s the vortex response is dominated by the trapped field and becomes independent of the applied field, thus, $B^* \approx B_s$.

To gain better insight into the structure of the critical state at low fields and the interplay between the self-field saturation field, B_s , and the crossover field to the single-vortex pinning, B_0 , we modeled our data using the procedure and MATLAB code developed by E. H. Brandt.^{15,21} This code computes the evolution of the current/field distribution and of the magnetization with field sweep for the critical state in a rectangular sample for arbitrary magnetic field dependence of the critical current. In our situation the field dependence at high fields is given by the power law, $J_c(B) = J_c(0)(B_0/B)^\alpha$ while at small fields it is masked by the self-field effects. In the case $B_0 < B_{s0} = \mu_0 J_{c0} t$ saturation of the critical current with decreasing magnetic field takes place in the field range, where the power-law dependence is still valid. In this case, the saturation field B^* and the apparent low-field value of the critical current J_{c0} can be estimated as $B^* \approx B_s = B_{s0}(B_0/B_{s0})^\beta$ and $J_{c0} \approx J_c(0)(B_0/B_{s0})^\beta$ with $\beta = \alpha/(1 + \alpha) \approx 1/3$ for $\alpha \approx 1/2$. We found that a good description of the data can be achieved assuming the field dependence of J_c in the form $J_c(B) = J_c(0)/[1 + (B/B_0)^2]^{\alpha/2}$. The fits of the data in Fig. 3(a) yield that $J_c(0)$ is larger than J_{c0} by about 10% and that

the fraction B_0/B_{s0} increases from 0.4 in the pristine sample to 0.64 in 7×10^{16} sample. Using the experimental dose dependence of J_c , $J_c \sim c\sqrt{n_p}/\sqrt{B}$, one also finds that due to self-field effects J_{c0} increases as $J_{c0} = J_c(B^*) \sim (n_p)^{1/3}$. Within the scatter, the data in Fig. 4 are consistent with this evolution.

Fig. 3(b) shows the field-dependence of the critical current density of crystal B after various doses of p-irradiation. In contrast to the behavior of crystal A, p-irradiation does not induce a significant enhancement of the low field critical current density. At high fields, J_c rolls off; however, in the accessible field range we cannot establish a relation of the form $J_c \sim B^{-\alpha}$ at 5 K. As a guide, the dashed line in Fig. 3(b) indicates the $1/B$ -dependence that is expected for vortex pinning by parallel columnar defects.²² We use this dependence to extrapolate B^* -values at a temperature of 20 K and plot them in the inset of Fig. 4. The Pb and proton-irradiated crystal displays a larger field range of nearly field-independent J_c . This is in part due to self-field effects which are expected to be larger in crystal B as it is twice as thick as crystal A. However, as is evident from an inspection of the data in Fig. 3(b) and in the inset of Fig. 4, upon p-irradiation B^* increases by almost a factor of two, whereas J_{c0} is constant within the uncertainties. We therefore contend that the mixed pinning landscape composed of heavy ion tracks and p-irradiation induced random defects enables field independent pinning up to fields of almost 6 T.

Nevertheless, these values of B^* are substantially smaller than the dose-matching field of the columnar defects of $B_\phi = 21$ T. TEM studies⁶ have revealed that—just as in cuprate high- T_c superconductors—the spatial distribution of irradiation tracks in $\text{Ba}_{0.6}\text{K}_{0.4}\text{Fe}_2\text{As}_2$ is highly non-uniform. Work on pinning by random arrays of irradiation tracks in cuprates has shown²³ that vortex-vortex repulsion and crowding induces unoccupied tracks in areas of high track density and interstitial vortices in areas of sparse tracks even at fields well below B_ϕ , accompanied by a roll-off of J_c near a field of the order of $(1/3-1/2) B_\phi$. Pinning by more regular arrays of dislocations induces a roll-off near $\sim 0.7 B_\phi$.²⁴ In the framework of a mixed pinning landscape, the p-irradiation induced defects pin interstitial vortices, and at the same time, suppress the motion of vortex kinks that form between tracks.⁸ The contributions to pinning from p-irradiation induced defects on columnar defects are not simply additive; at low fields, vortices are strongly pinned by columnar defects and the addition of p-induced defects does not increase J_c strongly. In contrast, in high fields p-induced defects pin interstitial vortices and their contribution to the total pinning is roughly equal to that due to columnar defects (see Fig. 3(b)). We note that the critical current density of crystal B at 5 K and 7 T of 5 MA/cm² equals that of state-of-the-art YBCO coated conductors containing correlated pinning sites in the form of Barium zirconate (BZO) nano-rods at the same temperature and field.⁹

The evolution of the temperature dependence of J_c in 0.2 T and in 4 T of crystals A and B with p-irradiation is shown in Fig. 5 revealing that the features described above persist over the entire temperature range up to T_c . Proton-irradiation causes a large enhancement of J_c of the pristine sample at all temperatures. At high p-fluence $J_c(T)$ is almost linear over an extended temperature range. The dependence and the absolute J_c -values are very similar to those of the

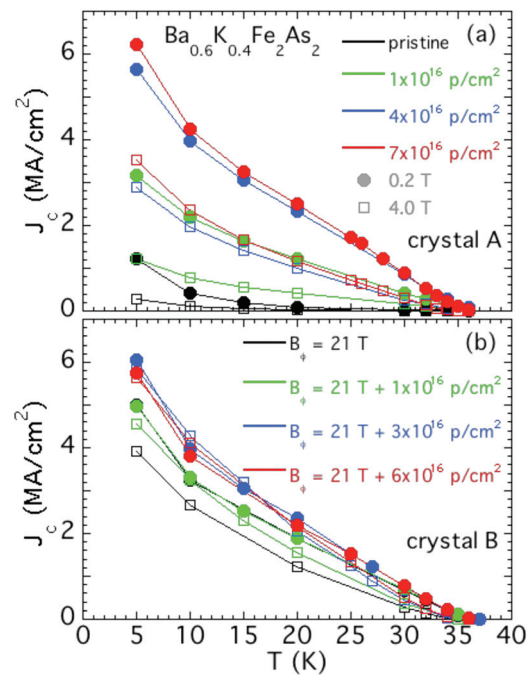


FIG. 5. (a) Temperature dependence of the critical current density of crystal A and of crystal B (panel (b)) for various p-fluences. Solid circles represent J_c in a field of 0.2 T and open squares in 4 T.

heavy-ion irradiated sample. As indicated by the spread of the curves in Fig. 5 and as noted above, the effect of composite heavy-ion tracks/random defects is enhanced pinning in high magnetic fields.

In conclusion, we carried out mixed pinning landscape studies of correlated and point defects induced by heavy-ion and proton irradiation in $\text{Ba}_{0.6}\text{K}_{0.4}\text{Fe}_2\text{As}_2$ single crystals. For both the mixed pinning landscape and the pure proton-induced pinning defects, we find a nearly field-independent enhancement of the critical current up to a threshold field, B^* . For the pure p-irradiated crystal, a comparison of the zero field J_c enhancement with B^* demonstrates that the extent of the field-independent J_c can be attributed to the onset of self-field effects. In contrast, for the mixed pinning landscape, the extent of the field independent J_c goes beyond the self-field effect and results in a nearly field independent J_c up to almost 6 T. Our measured critical current of 5 MA/cm² at 5 K and 7 T in single crystal form equals that of state-of-the-art YBCO coated conductors containing correlated pinning sites in the form of BZO nano-rods at the same temperature and field and indicates the potential applications of this material.

This work was supported by the Center for Emergent Superconductivity, an Energy Frontier Research Center funded by the U.S. Department of Energy, Office of Science, Office of Basic Energy Sciences (KK, LF, YJ, BS, AEK, UW, GWC, WKK). The operation of the ATLAS facility was supported by the U.S. Department of Energy, Office of Nuclear Physics, under Contract No. DE-AC02-06CH11357 (SZ). Proton-irradiation of the samples was carried out at the Western Michigan University accelerator laboratory (AK). The work in China was supported by the NSF of China, the MOST of China (Nos. 2011CBA00102 and 2012CB821403) and PAPD (HHW).

- ¹A. Gurevich, *Nature Mater.* **10**, 255 (2011).
- ²M. Rotter, M. Tegel, and D. Johrendt, *Phys. Rev. Lett.* **101**, 107006 (2008).
- ³H. Q. Yuan, J. Singleton, F. F. Balakirev, S. A. Baily, G. F. Chen, J. L. Luo, and N. L. Wang, *Nature* **457**, 565 (2009).
- ⁴Z.-S. Wang, H.-Q. Luo, C. Ren, and H.-H. Wen, *Phys. Rev. B* **78**, 140501 (2008); U. Welp, R. Xie, A. E. Koshelev, W. K. Kwok, H. Q. Luo, Z. S. Wang, G. Mu, and H. H. Wen, *ibid.* **79**, 094505 (2009).
- ⁵J. D. Weiss, C. Tarantini, J. Jiang, F. Kametani, A. A. Polyanskii, D. C. Larbalestier, and E. E. Hellstrom, *Nature Mater.* **11**, 682 (2012); Y. Ma, *Supercond. Sci. Technol.* **25**, 113001 (2012).
- ⁶L. Fang, Y. Jia, C. Chaparro, G. Sheet, H. Claus, M. A. Kirk, A. E. Koshelev, U. Welp, G. W. Crabtree, W. K. Kwok, S. Zhu, H. F. Hu, J. M. Zuo, H.-H. Wen, and B. Shen, *Appl. Phys. Lett.* **101**, 012601 (2012).
- ⁷T. Tamegai, T. Taen, H. Yagyu, Y. Tsuchiya, S. Mohan, T. Taniguchi, Y. Nakajima, S. Okayasu, M. Sasase, H. Kitamura *et al.*, *Supercond. Sci. Technol.* **25**, 084008 (2012).
- ⁸B. Maiorov, S. A. Baily, H. Zhou, O. Ugurlu, J. A. Kennison, P. C. Dowden, T. G. Holesinger, S. R. Foltyn, and L. Civale, *Nature Mater.* **8**, 398 (2009); J. Hua, U. Welp, J. Schlueter, A. Kayani, Z. L. Xiao, G. W. Crabtree, and W. K. Kwok, *Phys. Rev. B* **82**, 024505 (2010).
- ⁹M. Miura, B. Maiorov, S. A. Baily, N. Haberkorn, J. O. Willis, K. Marken, T. Izumi, Y. Shiohara, and L. Civale, *Phys. Rev. B* **83**, 184519 (2011).
- ¹⁰Y. Jia, M. LeRoux, D. J. Miller, J. G. Wen, W. K. Kwok, U. Welp, M. W. Rupich, X. Li, S. Sathyamurthy, S. Fleshler, A. P. Malozemoff, A. Kayani, O. Ayala-Valenzuela, and L. Civale, *Appl. Phys. Lett.* **103**, 122601 (2013); D. M. Feldmann, T. G. Holesinger, B. Maiorov, H. Zhou, S. R. Foltyn, J. Y. Coulter, and I. Apodoca, *Supercond. Sci. Technol.* **23**, 115016 (2010).
- ¹¹C. P. Bean, *Phys. Rev. Lett.* **8**, 250 (1962); *Rev. Mod. Phys.* **36**, 31 (1964).
- ¹²L. Civale, A. D. Marwick, M. W. McElfresh, T. K. Worthington, A. P. Malozemoff, F. H. Holtzberg, J. R. Thompson, and M. A. Kirk, *Phys. Rev. Lett.* **65**, 1164 (1990); M. A. Kirk, *Cryogenics* **33**, 235 (1993).
- ¹³M. A. Kirk and Y. Yan, *Micron* **30**, 507 (1999).
- ¹⁴C. J. van der Beek, G. Rizza, M. Konczykowski, P. Fertey, I. Monnet, T. Klein, R. Okazaki, M. Ishikado, H. Kito, A. Iyo, H. Eisaki, S. Shamoto, M. E. Tillman, S. L. Bud'ko, P. C. Canfield, T. Shibauchi, and Y. Matsuda, *Phys. Rev. B* **81**, 174517 (2010).
- ¹⁵G. P. Mikitik and E. H. Brandt, *Phys. Rev. B* **62**, 6800 (2000).
- ¹⁶T. Taen, T. Ohori, F. Ohtake, T. Tamegai, K. Kihou, S. Ishida, H. Eisaki, and H. Kitamura, *Physica C* **494**, 106 (2013).
- ¹⁷A. E. Koshelev and A. B. Koltun, *Phys. Rev. B* **84**, 104528 (2011).
- ¹⁸Yu. N. Ovchinnikov and B. I. Ivlev, *Phys. Rev. B* **43**, 8024 (1991); C. J. van der Beek, M. Konczykowski, A. Abaloshev, I. Abalosheva, P. Gierlowski, S. J. Lewandowski, M. V. Indenbom, and S. Barbanera, *ibid.* **66**, 024523 (2002); G. Blatter, V. B. Geshkenbein, and J. A. G. Koopmann, *Phys. Rev. Lett.* **92**, 067009 (2004).
- ¹⁹Y. Nakajima, T. Taen, Y. Tsuchiya, T. Tamegai, H. Kitamura, and T. Murakami, *Phys. Rev. B* **82**, 220504 (2010).
- ²⁰M. Däumling and D. C. Larbalestier, *Phys. Rev. B* **40**, 9350 (1989); L. W. Conner and A. P. Malozemoff, *ibid.* **43**, 402 (1991); H. P. Wiesinger, F. M. Sauerzopf, and H. W. Weber, *Physica C* **203**, 121 (1992); A. A. Babaei Brojeny and J. R. Clem, *Supercond. Sci. Technol.* **18**, 888 (2005); F. Hengstberger, M. Eisterer, and H. Weber, *Appl. Phys. Lett.* **96**, 022508 (2010); O. Polat, J. W. Sinclair, Y. L. Zuev, J. R. Thompson, D. K. Christen, S. W. Cook, D. Kumar, Y. Chen, and V. Selvamanickam, *Phys. Rev. B* **84**, 024519 (2011).
- ²¹E. H. Brandt, *Phys. Rev. B* **52**, 15442 (1995); *Phys. Rev. Lett.* **74**, 3025 (1995); Th. Schuster, H. Kuhn, E. H. Brandt, M. V. Indenbom, M. Leghissa, M. Kraus, M. Kläser, G. Müller-Vogt, H.-U. Habermeier, H. Kronmüller, and A. Forkl, *Phys. Rev. B* **52**, 10375 (1995).
- ²²D. R. Nelson and V. M. Vinokur, *Phys. Rev. B* **48**, 13060 (1993).
- ²³L. Civale, A. D. Marwick, T. K. Worthington, M. A. Kirk, J. R. Thompson, L. Krusin-Elbaum, Y. Sun, J. R. Clem, and F. Holtzberg, *Phys. Rev. Lett.* **67**, 648 (1991); L. Civale, *Supercond. Sci. Technol.* **10**, A11 (1997); L. Krusin-Elbaum, L. Civale, J. R. Thompson, and C. Field, *Phys. Rev. B* **53**, 1144 (1996); M. Konczykowski, F. Rullier-Albenque, E. R. Yacoby, A. Shaulov, Y. Yeshurun, and P. Lejay, *ibid.* **44**, 7167 (1991); K. Itaka, T. Shibauchi, M. Yasugaki, T. Tamegai, and S. Okayasu, *Phys. Rev. Lett.* **86**, 5144 (2001).
- ²⁴B. Dam, J. M. Huijbregtse, F. C. Klaassen, R. C. F. van der Geest, G. Doornbos, J. H. Rector, A. M. Testa, S. Freisem, J. C. Martinez, B. Stauble-Pumpin, and R. Griessen, *Nature* **399**, 439 (1999).